Spectroscopic and Theoretical Study of the Electronic Structure of Curcumin and Related Fragment Molecules

V. Galasso*

Dipartimento di Scienze Chimiche, Università di Trieste, I-34127 Trieste, Italy

B. Kovač

The Ruđer Bošković Institute, HR-10002, Zagreb, Croatia

A. Modelli

Dipartimento di Chimica "G. Ciamician", Università di Bologna, I-40129 Bologna, Italy, and Centro Interdipartimentale di Ricerca in Scienze Ambientali, Università di Bologna, I-48100 Ravenna, Italy

M. F. Ottaviani

Istituto di Scienze Chimiche, Università di Urbino, I-61029 Urbino, Italy

F. Pichierri

Department of Applied Chemistry, Graduate School of Engineering, Tohoku University, Aoba-yama 6-6-07, Sendai 980-8579, Japan

Received: November 13, 2007; In Final Form: December 19, 2007

The low volatility and thermal instability made the photoelectron (PE), electron transmission (ET), and dissociative electron attachment (DEA) spectroscopy measurements on curcumin (a potent chemopreventive agent) unsuccessful. The filled and empty electronic structure of curcumin was therefore investigated by exploiting the PES, ETS, and DEAS results for representative fragment molecules and suitable quantum-mechanical calculations. On this basis, a reliable pattern of the vertical ionization energies and electron attachment energies of curcumin was proposed. The π frontier molecular orbitals (MOs) are characterized by sizable interaction between the two phenol rings transmitted through the dicarbonyl chain and associated with a remarkably low ionization energy and a negative electron attachment energy (i.e., a largely positive electron affinity), diagnostic of a stable anion state not observable in ETS. The lowest energy electronic transitions of half-curcumin and curcumin and their color change by alkalization were interpreted with time-dependent density functional theory (DFT) calculations. For curcumin, it is shown that loss of a phenolic proton occurs in alkaline ethanolic solution.

Introduction

Curcumin, 1,7-bis(4-hydroxy-3-methoxyphenyl)-1,6-heptadiene-3,5-dione (**CU**, Figure 1), the yellow pigment of food flavoring turmeric and curry, is attracting remarkable continuing interest because of its antioxidant, anti-inflammatory, and potential cancer chemo-preventive activities.[1−5] Recently, it has also been proven that **CU** binds to β-amyloid aggregates in models of Alzheimer's disease.[6,7] Because the various mechanisms of biological action of a drug molecule are closely related to its electronic structure, a thorough experimental and theoretical investigation on such aspects of **CU** seems therefore timely.

Among the various spectroscopic observables, the vertical ionization energies (E_is) and electron attachment energies (VAEs) are efficient monitors of the complex interplay of structural and electronic effects operating in a molecule. Here, we describe measurements and quantum-mechanical calculations of these properties for simple reference molecules and **CU**. In particular, photoelectron spectroscopy (PES), electron transmission spectroscopy (ETS), and dissociative electron attachment spectroscopy (DEAS) are employed to experimentally probe the filled and empty electronic structures. These complementary data provide valuable information, especially about the energy and nature of the frontier molecular orbitals (MOs) that are primarily involved in the (bio)chemical reactivity of a compound.

Unfortunately, it must be remarked that our PES, ETS, and DEAS measurements on **CU** failed as a consequence of its low volatility and molecular decomposition upon heating at various temperatures up to a maximum of 230 °C. In this regard, we point out that the thermal instability of **CU** at these temperatures unexpectedly contradicts previous claims that **CU** is "thermally stable up to 249 °C both in static air and inert dynamic argon atmosphere".[8] In order to overcome this experimental drawback at least partially, we resorted to spectroscopic investigation of selected simple compounds, namely, guaiacol (**G**), *p*-vinyl-guaiacol (**VG**), and dehydrozingerone (**DHZ**, also referred to as half-curcumin), that may be viewed as fragment units of **CU** (Figure 1). On this experimental basis and with the support of

* To whom correspondence should be addressed. E-mail: galasso@univ.trieste.it.

10.1021/jp7108303 CCC: $40.75
Published on Web 02/16/2008

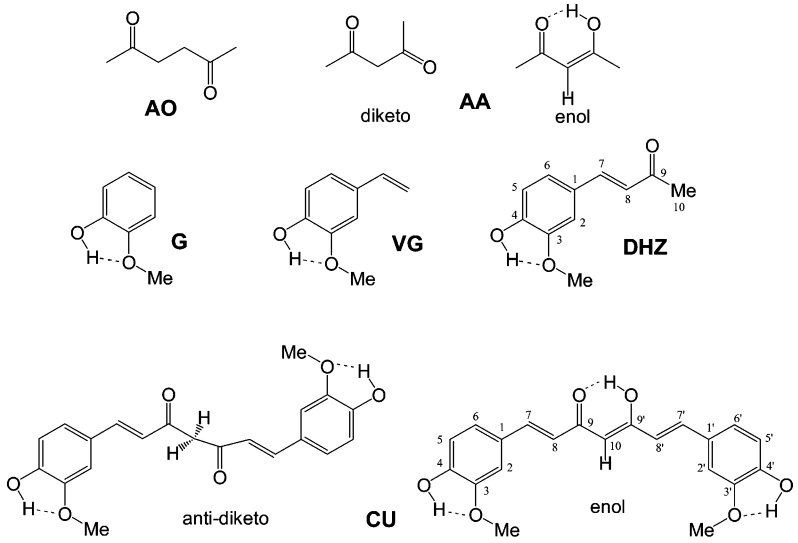

Figure 1. Molecular formulas and labeling.

accurate quantum-mechanical calculations, we then predict a reasonable pattern of the E_is and VAEs of **CU**. The main bands of the electronic absorption spectra of **DHZ** and **CU** and their color change by alkalization have been interpreted with time-dependent density functional theory (TD-DFT) calculations.

In the literature, there are a few quantum-mechanical studies devoted to theoretical elucidation of the molecular structure, absorption spectra, and antioxidant properties of **CU**.[9−19]

Experimental and Computational Details

The He(I) PE spectra were recorded on a Vacuum Generators UV-G3 spectrometer[20] with a spectral resolution of 25 meV when measured at the full width at half-maximum of the Ar^+ $^2P_{3/2}$ calibration line. The sample inlet temperatures required to generate sufficient vapor pressure were 30, 65, and 120 °C, for **G**, **VG**, and **DHZ**, respectively. The energy scale was calibrated by admitting small amounts of Ar and Xe to the sample flow.

The VAEs of **G**, **VG**, **DHZ**, and the reference molecules acetonylacetone (**AO**) and acetylacetone (**AA**) were measured by means of ETS. Our experimental setup is in the format devised by Sanche and Schulz[21] and has been previously described.[22] To enhance the visibility of the sharp resonance structures, the impact energy of the electron beam is modulated with a small ac voltage, and the derivative of the electron current transmitted through the gaseous sample is measured directly by a synchronous lock-in amplifier. Each resonance is characterized by a minimum and maximum in the derivative signal. The energy of the midpoint between these features is assigned to the VAE. The spectra were obtained in the "high-rejection" mode[23] and are therefore related to the nearly total scattering cross-section. The electron beam resolution was about 50 meV (fwhm). The energy scale was calibrated with reference to the $(1s^12s^2)^2S$ anion state of He. The estimated accuracy of the measured VAEs is ±0.05 or ±0.1 eV, depending on the number of decimal digits reported. The collision chamber of the ETS apparatus has been modified[24] in order to allow for ion extraction at 90° with respect to the electron beam direction. These ions are then accelerated and focused toward the entrance of a quadrupole mass filter. Alternatively, the total anion current can be collected and measured (with a picoammeter) at the walls of the collision chamber (about 0.8 cm from the electron beam). The DEAS data reported here were obtained with an electron beam current about twice as large as that used for the ETS experiment. The energy spread of the electron beam increased to about 100 meV, as evaluated from the width of the SF_6^- signal at zero energy used for calibration of the energy scale.

All compounds were obtained from a commercial source (Aldrich Co.) and used as received.

The vertical E_is of **G**, **VG**, **DHZ**, **CU**, and reference molecules were calculated at the ab initio level according to Cederbaum's outer-valence-Green's-function (OVGF) method,[25] which incorporates the effects of electron correlation and reorganization beyond the Hartree−Fock (HF) approximation. The self-energy part was expanded up to third order, and the contributions of higher orders were estimated by means of a renormalization procedure. In order to calculate the self-energy part, all occupied valence MOs and the 60 (**G**), 75 (**VG**), 90 (**DHZ**), and 170 (**CU**) lowest virtual MOs were considered. The OVGF calculations were performed using the TZV basis set[26] and molecular structures optimized at the DFT/B3LYP level of theory.[27]

Vertical excitation energies and oscillator strengths were calculated with the TD-DFT method,[28] employing the B3LYP functional and the cc-pVDZ basis set, augmented with sp diffuse functions[29] on the heavy atoms in the case of the anionic species. Solvent effects were accounted for with the polarizable continuum model (PCM).[30]

All quantum-mechanical calculations were carried out with the Gaussian 03 package of programs.[31]

Results and Discussion

Before starting the discussion, it must be recalled that the chemical structure of **CU** consists of two methoxyphenol rings connected by a conjugated dicarbonyl backbone. From a qualitative standpoint, **CU** can be regarded as being composed of two planar half-curcumin (**DHZ**) units. However, the resulting β-diketo moiety preferentially adopts the syn keto−enol form, which is favored by a strong intramolecular hydrogen bond (O···H 1.54 Å) over the anti β-diketo form (by 6.23 kcal mol^{-1} according to our DFT calculations). Whereas the syn keto−enol form is planar (C_s symmetry), the two halves of the conjugated framework are instead twisted by 73° in the anti β-diketo form (C_2 symmetry). X-ray crystal structure analyses[32,33] and NMR studies[34] of **CU** have established that the keto−enol structure exists in the solid state and is strongly favored in solution.

Ionization Energies. The following aspects of the filled electronic structure of **CU** in the low-energy region are of special

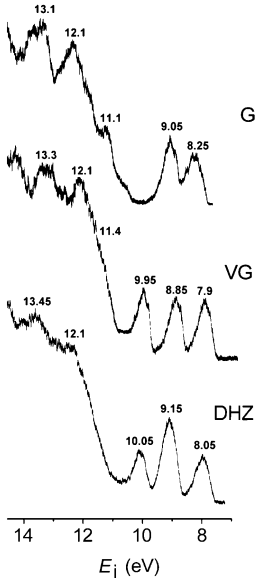

Figure 2. He(I) photoelectron spectra of compounds **V**, **VG**, and **DHZ**.

TABLE 1: Vertical Ionization Energies (eV) and Assignment

AA (enol)			**AA** (diketo)		
MO	$E_{i,calcd}$	$E_{i,exp}$	MO	$E_{i,calcd}$	$E_{i,exp}$
$\pi_{C=C}$	8.67	9.08[a]	n_O^-	9.79	9.63[a]
n_{Ok}	10.02	9.63	n_O^+	10.35	10.16
$\pi_{C=O}$	12.52	12.5	$\pi_{C=O}^+$	12.80	
n_{Oe}	13.06		$\pi_{C=O}^-$	12.92	12.9
π	13.36	13.2	σ	13.18	

G			VG		
MO	$E_{i,calcd}$	$E_{i,exp}$	MO	$E_{i,calcd}$	$E_{i,exp}$
π_S	7.94	8.25[b]	π_S	7.53	7.9[b]
π_A	8.77	9.05	π_A	8.67	8.85
π	11.39	11.1	$\pi_{C=C}$	10.00	9.95
σ	12.02	12.1	π	11.88	11.4
σ	12.36		σ	11.96	12.1

DHZ [enol][c]			**CU** [diketo][d]		
MO	$E_{i,calcd}$	$E_{i,exp}$	MO	$E_{i,calcd}$	$E_{i,exp}$
π_S	7.65 [7.17][c]	8.05[b]	π	7.15 [7.62][d]	(7.6)[e]
π_A	8.88 [8.53]	9.15	π	7.63 [7.64]	(8.0)
n_{Ok} [$\pi_{C=C}$][c]	9.57 [8.90]		π	8.54 [8.85]	(8.9)
$\pi_{C=C}$	9.98 [10.25]	10.05	π	8.81 [8.86]	(9.2)
π	12.07 [11.83]	12.1	$\pi_{C=C}$ [n_O^-][d]	8.87 [9.30]	(9.0)
σ	12.14 [11.90]		n_{Ok} [n_O^+]	9.70 [9.88]	(9.3)
σ	12.37 [12.03]		$\pi_{C=C}^{\pm}$	9.85 [9.94]	(10.0)
π	12.54 [12.56]		$\pi_{C=C}^{\pm}$	10.13 [9.96]	(10.2)
π[σ]	12.80 [12.91]		π	11.91 [11.98]	(12.0)
σ	13.14 [12.95]		π	11.99 [12.00]	

[a] Reference 39. [b] This work. [c] Theoretical values for the enol form of **DHZ**. [d] Theoretical values for the diketo form of **CU**. [e] In parentheses, tentative expectation values for the enol form of **CU**.

interest: (i) the location and formal splitting of the n E_is associated with the carbonyl lone-pair orbitals n_O, (ii) the sequence and composition of the uppermost π E_is, and (iii) the location of the ethenic π E_is. This information can be extracted from the He(I) PE spectra of the 'fragment molecules' (Figure 2) and related quantum-mechanical calculations. The relevant experimental E_is together with the ab initio many-body OVGF results are reported in Table 1. For the sake of simplicity, some assignments are described with reference to the predominant character of the MO involved, in particular, n_O, π(phenolic), $\pi_{C=C}$, and $\pi_{C=O}$. The pole strengths calculated for all investigated photoionization processes are larger than 0.85, which excludes the presence of nearby shakeup lines and thus indicates that the one-particle model of ionization is valid.[35−37]

The results obtained by means of the same OVGF approach for some small, related molecules were used as a yardstick for the assignments of the PE spectra of **G**, **VG**, and **DHZ**. The molecules taken into account are the following: **AO** (hexane-2,5-dione), **AA** (pentane-2,4-dione), phenol, anisole, and styrene.

In the low-energy region of the PE spectrum, the γ-dicarbonyl **AO** exhibits one band centered at 9.63 eV that is assigned to the almost degenerate pair n_O^+ and n_O^-.[34] Consistently, our ab initio OVGF calculations yield the sequence n_O^+, n_O^-, $\pi_{C=O}^-$, and $\pi_{C=O}^+$, with relevant values 9.88, 10.03, 12.42, and 12.67 eV. Notably, by exploiting variable-temperature PES, Hush et al.[39] obtained the complete spectra of both tautomers of **AA** with a $\pi_{C=C} < n_O < \pi_{C=O}$ sequence for the enol tautomer and $n_O^- < n_O^+ < \pi_{C=O}^+$ for the keto tautomer. Interestingly, our OVGF results for **AA** are in good agreement with experiment (Table 1). Furthermore, as concerns the benzenoid molecules, the correspondence between experiment and theory is satisfactory. Indeed, the first E_is of phenol are observed[40] at 8.67, 9.36, 11.50, 12.0, and 12.6 eV and predicted by OVGF theory at 8.39 (π_S), 9.16 (π_A), 11.82 (π), 12.05 (n), and 12.69 (σ) eV. (Here, the assignments indicate the predominant character of the MO involved; in particular, π_S and π_A represent the symmetric and antisymmetric, respectively, components of the parental benzene e_{1g} HOMO.) For anisole, the OVGF results are 8.19 (π_S), 9.05 (π_A), 11.33 (π), 11.58 (n), and 12.48 (σ) eV and the experiment[40] yields the corresponding E_is of 8.42, 9.21, 11.02, 11.60, and 12.4 eV. For styrene, the OVGF results are 8.20 (π_S), 9.00 (π_A), 10.65 (π_{CC}), 11.81 (σ), and 11.97 (σ) eV versus the spectroscopic values[41] of 8.47, 9.27, 10.56, 11.51, and 12.17 eV. Therefore, the theoretical formalism employed here suffers from a slight underestimation of the top phenyl $\pi_{S,A}$ E_is, while it reproduces the n_O and π_{CC} E_is within 0.1−0.4 eV.

With this background information, the ab initio OVGF results reported in Table 1 allow for consistent assignments of the PE spectra of **G**, **VG**, and **DHZ**. In particular (Figure 2), in the PE spectrum of **DHZ**, which exists exclusively in the keto form, the first band at 8.05 eV is generated by photoionization from the top π(methoxyphenolic) MO, the second band peaked at 9.15 eV comprises photoionization both from another outermost π(methoxyphenolic) MO and from the n_O of the carbonyl group, and photoionization from the π ethenic (π_{CC}) MO gives rise to the third band centered at 10.05 eV. After a gap of 1 eV, there is the onset of a prominent band system that encompasses a manifold of closely lying photoionizations of π_{CO}, σ, and n_O (phenolic) character.

Formal connection of the (real) keto and (virtual) enol tautomers of **DHZ** gives the lowest energy (enol/keto) tautomer of **CU**. On the other hand, formal dimerization of the keto tautomer of **DHZ** generates the less stable (diketo) tautomer of **CU**. Both of these fusions are accompanied by doubling of the n_O, π(methoxyphenolic), π(carbonyl), and π(ethenic) semilocalized MOs, which now interact through space and through bond. As can be seen from the OVGF results reported in Table 1, there is a clear correlation between the MOs of the **DHZ** precursor moieties and the corresponding MO pairs in the two 'composite' tautomers of **CU**. Therefore, by qualitative perturbative arguments, slight destabilization and splitting of the MOs, which span the entire molecule **CU**, are expected in all cases (see Table 1 and the partial correlation diagram given in Figure 3). This energetic pattern indicates that the heptadienone chain behaves as a moderately efficient electronic relay between the

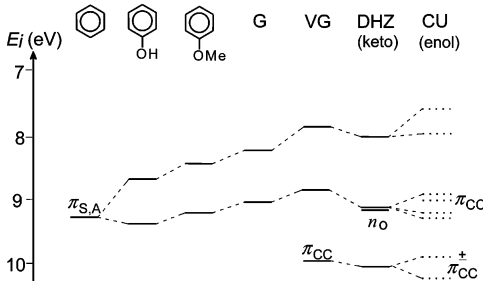

Figure 3. Partial correlation diagram of experimental (continuous lines) and expected (dashed lines) E_is.

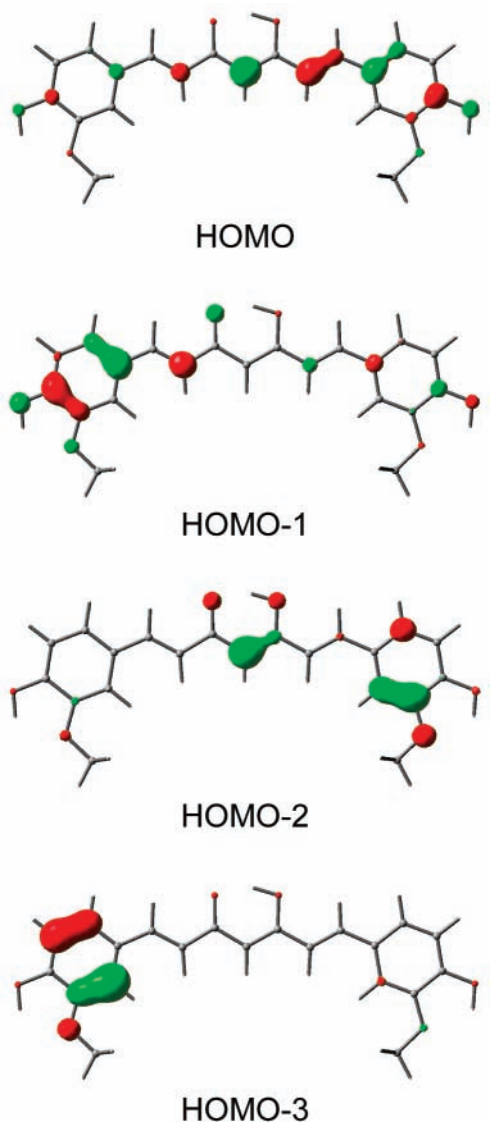

Figure 4. Representation of the top occupied MOs of **CU** (enolic form).

two distant methoxyphenolic rings of **CU**. As illustrative examples, the four top occupied π MOs of **CU** are shown in Figure 4.

In conclusion, by taking into account the consistent orbital sequence and assignments achieved for the 'fragment molecules', a reasonably accurate prediction can be advanced for the low-energy photoionizations of **CU**: the relevant E_i values are reported (in parentheses) in the last column of Table 1. A notable aspect, which is directly connected with the molecular reactivity, is the remarkably low first vertical E_i expected for **CU**, about 7.6 eV.

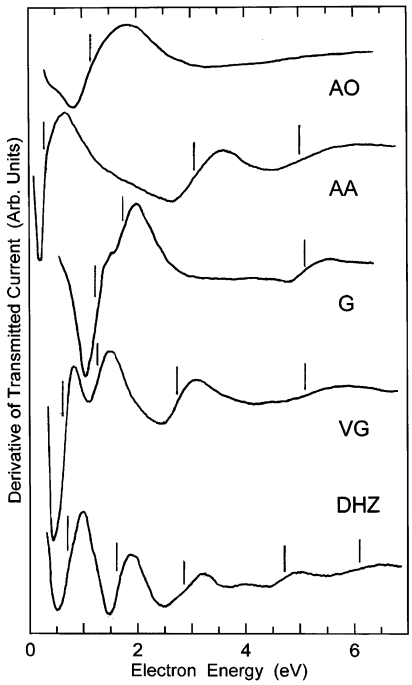

Figure 5. Derivative of transmitted current, as a function of electron energy, in **AO**, **AA**, **G**, **VG**, and **DHZ**. Vertical lines locate the VAEs.

Electron Attachment Energies. Because electron attachment is rapid with respect to nuclear motion, temporary anions are formed in the equilibrium geometry of the neutral molecule. The impact electron energies at which electron attachment occurs are properly denoted as vertical attachment energies (VAEs) and are the negative of the vertical electron affinities. Figure 5 reports the ET spectra of **AO**, **AA**, **G**, **VG**, and **DHZ**. The measured VAEs are given in Table 2 together with the π^* virtual orbital energies (VOEs) of the neutral state molecules supplied by HF/6-31G and B3LYP/6-31G(d) calculations.

A theoretical approach adequate for describing the energetics of the unstable anion states observed in ETS involves difficulties not encountered for neutral or cation states. The first VAE can, in principle, be obtained as the energy difference between the lowest-lying anion and the neutral state (both with the optimized geometry of the neutral species). A proper description of the spatially spread electron distribution of anions requires a basis set with diffuse functions.[42] However, as the basis set is expanded, an SCF calculation ultimately describes a neutral molecule and an unbound electron in as much of the continuum as the basis set can emulate. These low-energy solutions have no physical significance with regard to anion formation,[43−47] and the dependence of the calculated energies and localization properties on the addition of diffuse function to the basis set increases with increasing anion state instability.[48] However, it has been shown that simple Koopmans' theorem (KT) calculations, using empirical linear scalings, can satisfactorily reproduce the π^* VAEs measured in a large number of systems containing various functionals and heteroatoms.[43,44,49]

Here, this simple and reliable procedure is used to support the association of the resonances observed in the ET spectra of the compounds investigated with the corresponding empty π^* MOs. In fact, systematic ETS studies have shown that empty σ^* MOs in unsaturated hydrocarbons give rise to distinct low-energy features in the ET spectra only in derivatives of third-row (or heavier) elements.[50] In addition, this procedure allows evaluating the energies of stable anion states (not observable in ETS) of **CU**. The empirical linear equations used to scale

TABLE 2: Virtual Orbital Energies (VOEs) Supplied by HF/6-31G and B3LYP/6-31G(d) Calculations and Experimental VAEs (All Values in eV); Scaled VOEs (See Text) in Parentheses

		VOE/HF	VOE/B3LYP	VAE
benzene	π^* b_{2g}	9.94 (5.01)	4.46 (4.80)	4.82[a]
	π^* e_{2u}	4.03 (1.15)	0.10 (1.29)	1.12
AO	$\pi^*_{CO}{}^+$	4.07 (1.18)	−0.31 (0.96)	
	$\pi^*_{CO}{}^-$	3.94 (1.09)	−0.44 (0.86)	1.15
AA (diketo)	$\pi^*_{CO}{}^-$	4.53 (1.47)	0.03 (1.24)	3.07
	$\pi^*_{CO}{}^+$	2.96 (0.45)	−1.23 (0.22)	0.30
AA (enol)	$\pi^*_{CC} - \pi^*_{CO}$	6.44 (2.72)	1.98 (2.80)	3.07
	$\pi^*_{CO,COH}$	2.79 (0.34)	−1.12 (0.31)	0.30
G	π^*_O	10.39 (5.30)	4.91 (5.16)	5.1
	π^*_S	4.37 (1.37)	0.58 (1.68)	1.74
	π^*_A	4.02 (1.14)	0.32 (1.47)	1.22
VG	π^*_O	10.72 (5.51)	5.12 (5.34)	5.1
	$\pi^*_{CC} - \pi^*_S$	6.40 (2.70)	2.00 (2.83)	2.74
	π^*_A	4.01 (1.14)	0.32 (1.47)	1.24
	$\pi^*_S + \pi^*_{CC}$	3.17 (0.59)	−0.58 (0.75)	0.52
DHZ	π^*_O	10.33 (5.34)	4.70 (5.00)	4.67
	$\pi^*_{CC} - \pi^*_{CO}$	6.77 (2.94)	2.32 (3.08)	2.84
	π^*_S, π^*_{CO}	4.77 (1.63)	0.64 (1.73)	1.63
	π^*_A	3.76 (0.97)	−0.03 (1.19)	0.73
	$\pi^*_{CO} + \pi^*_{CC}$	1.81 (−0.30)	−1.66 (−0.13)	≤0
CU (enol)	π^*_O	10.43 (5.04)	4.94 (5.06)	
	π^*_O	10.41 (5.03)	4.88 (5.01)	
	π^*_{CC}	8.58 (3.93)	3.71 (4.07)	
	π^*_{CC}	7.19 (3.09)	2.57 (3.16)	
	π^*_S, π^*_{CC}	5.80 (2.26)	1.50 (2.30)	
	π^*_S, π^*_{CO}	4.39 (1.41)	0.51 (1.52)	
	π^*_A	3.83 (1.07)	0.09 (1.18)	
	π^*_A	3.73 (1.01)	0.01 (1.12)	
	$\pi^*_{CO} + \pi^*_S$	2.43 (0.23)	−1.01 (0.31)	
	$\pi^*_{CO} + \pi^*_{CC}$	1.06 (−0.59)	−2.06 (−0.53)	
CU (diketo)	π^*_O	10.35 (5.00)	4.87 (4.99)	
	π^*_O	10.32 (4.98)	4.84 (4.98)	
	$\pi^*_{CC} - \pi^*_{CO}$	6.83 (2.88)	2.43 (3.05)	
	$\pi^*_{CC} - \pi^*_{CO}$	6.45 (2.65)	2.24 (2.90)	
	$\pi^*_S + \pi^*_{CO}$	4.92 (1.73)	0.82 (1.77)	
	$\pi^*_S + \pi^*_{CO}$	4.36 (1.39)	0.43 (1.45)	
	π^*_A	3.75 (1.03)	0.01 (1.11)	
	π^*_A	3.71 (1.00)	−0.03 (1.09)	
	$\pi^*_{CO} + \pi^*_{CC}$	1.88 (−0.10)	−1.54 (−0.12)	
	$\pi^*_{CO} + \pi^*_{CC}$	1.27 (−0.47)	−1.99 (−0.48)	

[a] Experimental VAEs from ref 23.

the HF/6-31G and B3LYP/6-31G(d) VOEs are taken from the literature (refs 44 and 49, respectively).

In **AO**, the two π^*_{CO} MOs are expected to lie close in energy, their direct mixing being prevented by the two intermediate CH_2 groups. Consistently, the ET spectrum displays a single unresolved resonance, centered at 1.15 eV, somewhat broader than that observed in the spectra of monoketones.[49] An average VAE slightly smaller than that (1.31 eV) of acetone[51] is in line with a mutual electron-withdrawing inductive effect exerted by the two carbonyl groups. In agreement, the scaled VOEs predict an energy splitting of only 0.1 eV between the two π^*_{CO} VAEs and also nicely reproduce their absolute values (see Table 2 and the diagram of Figure 6).

For the diketo form of **AA**, both the HF and B3LYP calculations predict a significant mixing (through the CH_2 group) between the two π^*_{CO} MOs (the scaled VOEs of the in-phase and out-of-phase combinations are about 0.3 and 1.3 eV, respectively, see Table 2). For the enolic form of **AA**, however, the predicted energy splitting is sizably larger. The first scaled VOE is about the same, but the second one (2.8 eV), associated with an antibonding π^*_{CC}/π^*_{CO} combination, is much larger. The ET spectrum of **AA** displays two sharp resonances at 0.30 and 3.07 eV and a broader feature centered at 5.0 eV, the latter being likely due to a core excited resonance, i.e., electron capture

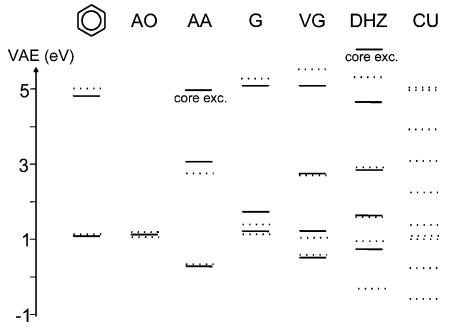

Figure 6. Experimental VAEs (continuous lines) and scaled HF/6-31G π VOEs (dashed lines).

accompanied by simultaneous excitation of a valence electron. The first two VAEs nicely match those predicted for the enolic form (Table 2), thus confirming the PES evidence[39] that this form of **AA** is largely prevailing in the gas phase.

In **G**, interaction with the oxygen lone pairs[50] removes the degeneracy of the benzene e_{2u} (π^*) lowest unoccupied MO (LUMO, VAE = 1.12 eV in benzene).[24] The two components (here denoted as π^*_A and π^*_S) give rise to the resonances located at 1.22 and 1.74 eV in the ET spectrum. The energy splitting predicted by the calculations is somewhat underestimated (see Table 2) although, due to partial overlap between the two resonances and the smaller intensity of the second one, the measured value of 1.74 eV could be an upper limit of the second VAE. The third resonance (5.1 eV) is associated with the MO deriving from the totally antibonding highest lying benzene b_{2g} (π^*) MO (denoted as π^*_O in Table 2), destabilized by mixing with the oxygen lone pairs.

Vinyl substitution in **G** to give **VG** introduces an additional empty π^*_{CC} MO (VAE = 1.73 eV in ethene).[52] The LUMO originates from strong (bonding) mixing between this MO and the lower lying ring π^*_S MO (which possesses a large wave function coefficient on the vinyl-substituted carbon atom). The ET spectrum of **VG** displays resonances at 0.52 and 2.74 eV associated with the LUMO and its antibonding counterpart π^* MO, respectively. In agreement, the corresponding anion states of styrene (where the destabilizing effect of the oxygen lone pairs is not present) are about 0.3 eV more stable.[52] The resonance associated with the nearly unperturbed (for symmetry reasons) benzene π^*_A MO is located at 1.24 eV. It is to be noted that, according to the calculations, in the most stable (coplanar) conformer of **VG** the vinyl group is rotated in the opposite direction with respect to the hydroxy and methoxy groups. However, the conformer with all three functionals rotated in the same direction is only 0.35 kcal/mol less stable (at the B3LYP/6-31G(d) level), so that the populations of the two conformers should be similar. The presence of the two conformers, however, is not expected to cause appreciable broadening of the spectral features because their corresponding scaled VOEs are calculated to be equal within experimental limits.

Carbonyl substitution at the vinyl group of **VG** gives **DHZ**. Because of the enlargement of the conjugated π system and the electron-withdrawing effect of the carbonyl group, the LUMO of **DHZ** (with mainly π^*_{CO} and π^*_{CC} character, see Figure 7) is clearly expected to be more stable than that of **VG**. Therefore, the first resonance (VAE = 0.73 eV) observed in the ET spectrum of **DHZ** is associated with electron capture into the second empty MO, with mainly benzene π^*_A character, electron capture into the LUMO giving rise either to a stable anion state (not detectable in ETS) or to an anion state so close (<0.2 eV) to zero energy to be masked by the intense incident electron beam signal. In agreement, the HF and B3LYP scaled

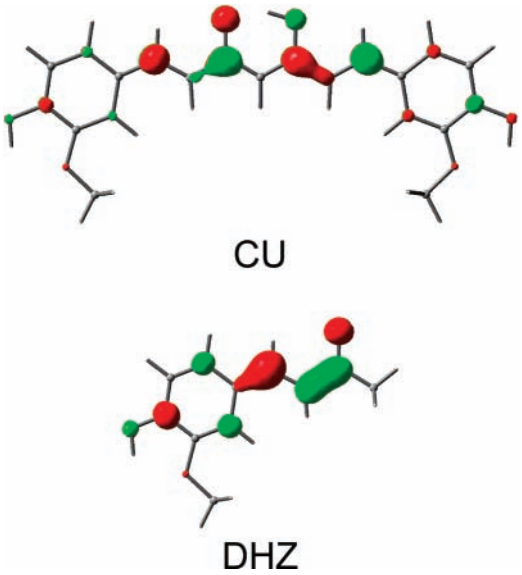

Figure 7. Representation of the LUMO of **DHZ** and **CU** (enolic form).

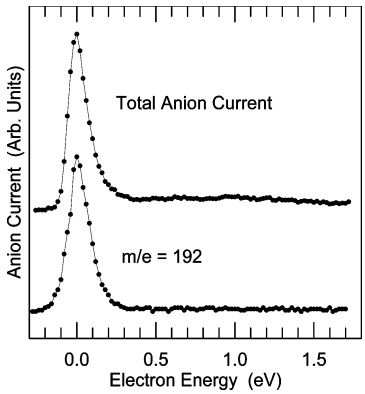

Figure 8. Total and mass-selected anion currents in **DHZ** as a function of incident electron energy.

VOEs (Table 2) predict the first anion state to be stable by about 0.2 eV (a negative VAE means a positive vertical electron affinity). The VAEs of the third and fourth π^* MOs of **DHZ** are closely reproduced by the scaled VOEs. It is worth noting that the measured VAE (4.67 eV) of the higher lying π^*_O MO is unexpectedly smaller than that of **VG** (and benzene). This can be partly due to the electron-withdrawing effect of the carbonyl group, but a major role is probably played by mixing with the higher lying (core-excited) anion state observed at 6.1 eV, this effect not being accounted for by KT calculations.

In order to achieve further experimental support to the predicted stability of the first vertical anion state of **DHZ**, the DEA spectra have been recorded, that is the anion current as a function of the incident electron energy has been measured. In the case of a slightly stable anion state, formation of the (vibrationally excited) molecular anions at thermal incident electron energies is expected to occur. When suitable energetic and kinetic conditions occur, the decay of the molecular anions can follow a dissociative channel which generates a long-lived negative fragment and a neutral radical, in kinetic competition with simple re-emission of the extra electron. The DEA spectra of **DHZ** in the 0−2 eV energy range are reported in Figure 8. The total anion current measured at the walls of the collision chamber (upper curve) displays an intense peak at zero energy, thus corroborating the theoretical prediction of a stable anion state. The negative current selected through a mass filter (lower curve) displays a zero energy peak at $m/e = 192$, corresponding to the parent molecular anion. Its lifetime, therefore, must be ≥ 1 μs, that is the survival time required to pass through the mass filter. Currents associated with negative fragments (generated by dissociation of the molecular anion) were not observed. Although the total anion current seems to display very weak signals around 0.6 and 1 eV, possibly due to dissociation of higher lying resonances, negative fragment currents were not observed through the mass filter, likely due to the smaller sensitivity of these measurements.

The reliability of the scaled VOEs in reproducing the VAEs measured in the smaller reference molecules gives confidence that the same approach is also suitable for evaluating the energies of the vertical anion states of the (preferred) *syn*-enolic form of curcumin (**CU**). However, in order to employ a plausibly even more accurate scaling, directly biased toward the functional groups which constitute **CU**, we determined linear relationships only from the data of the six (including benzene) reference molecules. The equations obtained (HF: VAE = 0.6017 VOE − 1.2323, $r^2 = 0.987$; B3LYP: VAE = 0.7985 VOE + 1.1098, $r^2 = 0.987$), rather close to those reported in the literature and used for the smaller molecules, lead to the VAEs of **CU** reported in Table 2 and the diagram of Figure 6. It can be noted that the two sets of values (HF and B3LYP) are equal within 0.1 eV.

A representation of the π^* LUMO of **CU** is shown in Figure 7. There is an important difference between the HOMO and LUMO of **CU**. The π HOMO encompasses the entire molecular framework with a large contribution from the central methine carbon atom and very small contributions from the oxygen atoms of the keto−enol moiety; the π^* LUMO is instead mainly localized on the central heptadienone chain in an antibonding manner and with a node on the methine carbon atom. As for the next π^* LUMOs of **CU**, the LUMO+1 is localized on the benzene rings and the intermediate carbon chain, while the LUMO+2 and LUMO+3 essentially possess only benzene character.

The vertical anion state associated with the LUMO of **CU** is predicted to be very stable (0.5−0.6 eV with both the B3LYP and HF scalings). The second anion state (with mainly ethene π^*_{CC} and benzene π^*_S character) is found to be somewhat unstable. Owing to its sizable stability, a proper description of the first anion state of **CU** should not require inclusion of diffuse functions in the basis set. To confirm the results obtained with the scaled VOEs, the difference between the total energies of the neutral state and the first anion state (both with the geometry optimized for the neutral molecule) has been calculated at the B3LYP/6-31G(d) level. The resulting vertical electron affinity is 0.78 eV, somewhat larger than that predicted by the scaling procedure. Geometry optimization of the anion state leads to an adiabatic electron affinity (0.91 eV) not much larger than the vertical electron affinity due to the relatively small geometrical changes caused by electron addition on this conjugated π system.

Electronic Transitions. The small HOMO−LUMO gap of **CU** explains its yellow color. Of course, the electronic structure of **CU** manifests itself in the entire absorption spectrum, which shows two prominent bands peaked at 427 and 265 nm in EtOH solution.[53,54] **CU** is a polytropic compound with three dissociable protons. A notable aspect is that in strongly basic media (e.g., $Ca(OH)_2$, NaOH, or KOH) **CU** undergoes deprotonation and the absorption spectrum of the resulting closed-shell anionic species $\mathbf{h_2Cu^-}$ exhibits a net bathochromic displacement, the color changing from yellow to purple.[17,19,53] The color change was also exploited to establish the site of donation of the proton,

TABLE 3: Electronic Transitions: Energies (eV and nm) and Intensities (Oscillator strength *f*, Molar Absorptivity ϵ)

	calcd			expt
assignment	E (eV)	λ (nm)	f	λ (ϵ)
		DHZ		
$n \rightarrow \pi^*$	3.62	342	0.0000	
$\pi \rightarrow \pi^*$	3.64	340	0.6208	337;[a] 340 (22 000)[b]
$\pi \rightarrow \pi^*$	4.21	294	0.1428	303 sh; 300 sh (10 000)
$\pi \rightarrow \pi^*$	5.01	248	0.0904	242
$\pi \rightarrow \pi^*$	5.49	226	0.1631	225
$\pi \rightarrow \pi^*$	5.75	216	0.0385	
$n \rightarrow \pi^*$	5.96	208	0.0004	
$n \rightarrow \pi^*$	6.30	197	0.0002	
		Dhz$^-$		
$\pi \rightarrow \pi^*$	3.06	405	1.0054	417 (34 000)[c]
$n \rightarrow \pi^*$	3.79	327	0.0000	
$\sigma \rightarrow \pi^*$	3.82	325	0.0000	
$\pi \rightarrow \pi^*$	4.05	306	0.0356	
$\pi \rightarrow \sigma^*$	4.26	291	0.0040	
$\pi \rightarrow \pi^*$	4.38	283	0.0578	
$\pi \rightarrow \sigma^*$	4.40	282	0.0001	
$\pi \rightarrow \sigma^*$	4.56	272	0.0009	
		CU		
$\pi \rightarrow \pi^*$	2.77	447	1.6888	427 (55 000)[b]
$\pi \rightarrow \pi^*$	3.20	387	0.0340	375 sh
$n \rightarrow \pi^*$	3.57	347	0.0000	
$\pi \rightarrow \pi^*$	3.73	332	0.0980	
$\pi \rightarrow \pi^*$	3.85	322	0.0130	
$\pi \rightarrow \pi^*$	4.02	308	0.0651	
$\pi \rightarrow \pi^*$	4.11	302	0.0619	
$\pi \rightarrow \pi^*$	4.27	290	0.2435	265 (22 000)[d]
$\pi \rightarrow \pi^*$	4.71	263	0.0216	
$\pi \rightarrow \pi^*$	4.74	261	0.0137	
		h_2Cu^-		
$\pi \rightarrow \pi^*$	2.27	547	1.6221	535 (59 400)[c]
$\pi \rightarrow \pi^*$	3.09	403	0.5490	450 sh
$\pi \rightarrow \pi^*$	3.45	360	0.0835	
$n \rightarrow \pi^*$	3.49	355	0.0000	
$\pi \rightarrow \pi^*$	3.61	344	0.0153	
$\sigma \rightarrow \pi^*$	3.73	332	0.0001	
$\pi \rightarrow \pi^*$	3.90	318	0.0205	
$\pi \rightarrow \pi^*$	4.01	310	0.0076	
$\pi^* \rightarrow \pi^*$	4.14	300	0.0289	
$\pi \rightarrow \sigma^*$	4.16	298	0.0025	

[a] In MeOH solution, ref 59. [b] In EtOH solution, ref 53. [c] In EtOH+KOH solution, ref 53. [d] In EtOH solution, ref 54.

either from one phenolic or the enolic group of **CU**, with controversial conclusions.[16,53,55−58]

Since **DHZ** formally represents one-half of the **CU** molecule, contains the same donor−acceptor chromophoric units, and exhibits a similar behavior by alkalization, examination of its absorption spectrum provides appropriate preliminary insight into that of **CU**. The UV spectrum of **DHZ** in MeOH solution shows a strong band at 340 nm, a distinct shoulder near 300 nm, and some other features at lower wavelengths.[53,59]

The TD-DFT/B3LYP/(aug-)cc-pVDZ results for the neutral and deprotonated anionic forms of **DHZ** and **CU** are listed in Table 3, together with the experimental results. In this respect, it is worthwhile to mention that previous reports place transition energies given by TD-DFT within approximately 0.3 eV of experimental values.[28,60,61] Furthermore, it must be stressed that the absorption spectra of the present compounds are strongly influenced by organic solvents, water, and pH (see, e.g., refs 53 and 62−65). In our calculations, the solvent (ethanol) effect was taken into account with the PCM formalism. On the whole, these DFT results are in substantial agreement with the spectroscopic data.

According to the TD-DFT results (Table 3), the lowest energy band of **DHZ** is generated by an intramolecular charge transfer from the aromatic ring (hosting the electron-donating groups −OH and −OMe) to the electron-acceptor carbonyl moiety: the associated π(HOMO) $\rightarrow$ π^*(LUMO) transition is polarized along the long axis of the molecule. The (virtually) dipole-forbidden $n \rightarrow \pi^*$(LUMO) transition is predicted to lie under the low-energy tail of the first strong band. The other features observed in the spectrum are ascribed to various $\pi \rightarrow \pi^*$ transitions. The TD-DFT results also account for the marked bathochromic shift (77 nm) shown by **DHZ** in ethanolic solution added with KOH,[53] changing from colorless to red as a result of formation of the anionic species **Dhz$^-$**.

For **CU**, the lowest energy band at 427 nm is associated with a strong electronic transition, whose major component is the π(HOMO) $\rightarrow$ π^*(LUMO) excitation involving a net intramolecular charge transfer from the two peripheral aromatic rings to the central α,γ-keto−enol moiety. Thus, there is a close parentage between the lowest energy bands of **DHZ** and **CU**, their excited singlet state being very polar. The weakly allowed π(HOMO-1) $\rightarrow$ π^*(LUMO) transition and the (virtually) forbidden $n \rightarrow \pi^*$(LUMO) transition should give rise to the shoulder found around 375 nm. The band at 265 nm can be attributed to the relatively intense π(HOMO-1) $\rightarrow$ π^*(LUMO+1) transition. A noteworthy point is that the present theoretical results show the inconsistencies in the former assignments based on naive FEMO and PPP calculations:[17,18] the visible band ascribed to the $n \rightarrow \pi^*$(LUMO) transition and the UV band to the π(HOMO) $\rightarrow$ π^*(LUMO) transition. On the other hand, the very low oscillator strength of the $n \rightarrow \pi^*$ transition should hardly be reconcilable with the strong absorption occurring at 427 nm. Furthermore, the present TD-DFT assignment agrees only partially with that recently given by Párkányi et al. with semiempirical PPP calculations[19] and is more complete than the DFT pattern reported by Shen and Li.[16]

As mentioned above, alkalization of **CU** should produce etherolitic breaking of the α,γ-keto−enol or a phenolic O−H bond. Note that the two equivalent asymmetric keto−enol tautomers of the phenolic **h_2Cu^-** species should rapidly interconvert in solution as established experimentally for the neutral compound.[34] According to our DFT(PCM) calculations, the enolic deprotonated anion of **CU** is 18.4 (in vacuo) and 12.6 (in EtOH solution) kcal mol^{-1} less stable than the phenolic one. In addition, the O−H bond dissociation enthalpy calculated for **CU** with the MLM2 method[66] is 83.0 (phenolic) and 106.6 (enolic) kcal mol^{-1}. These results indicate that the first dissociation of **CU** should involve a proton loss from one phenolic hydroxyl. The opposite conclusion claimed by Shen and Li ("the enolic proton is the most acidic one among the three dissociable protons in **CU**")[16] is devoid of energetic foundation. Accordingly, the TD-DFT results reported in Table 3 refer to the (averaged) phenolic **h_2Cu^-**. Consistent with experimental evidence (yellow to purple color change), on passing from **CU** to **h_2Cu^-**, the calculated electronic pattern undergoes a net bathochromic shift (100 nm), larger than that found in the case of **DHZ** (65 nm). Notably, deprotonation of the enolic OH of **CU** is calculated to cause a small displacement and a marked decrease of intensity for the first predicted $\pi \rightarrow \pi^*$ transition ($\lambda = 439$ nm, $f = 0.3839$). This theoretical output corroborates the conclusion of Zsila et al.[53] that dissociation of one phenolic OH is mainly responsible for the large red shift (108 nm) obtained by alkalization of **CU** in ethanolic solution.

Concluding Remarks

The electronic structure of **CU** could not be experimentally probed by means of PES, ETS, and DEAS because of the low

volatility and thermal instability of the compound. Nonetheless, a study of the filled and empty electronic structure of **CU** has been carried out by taking advantage of the corresponding spectroscopic results obtained for related 'fragment' molecules and suitable quantum-mechanical (ab initio OVGF and DFT) calculations. Thus, detailed assignments of the low-energy photoionization and electron attachment processes of **CU** have been proposed. The π frontier MOs of **CU** indicate a significant interaction between the two phenol halves through the dicarbonyl chain. A remarkably low E_i is associated with the HOMO. On the other hand, the LUMO is found to give rise to a sizably stable anion state. These electronic properties are diagnostic of a marked reactivity of **CU**, whose various pharmacological functions are attracting growing interest. The low-lying electronic excited states have been characterized in terms of the main one-electron jumps, and the color change observed in alkaline ethanolic solution has also been accounted for fairly well. In particular, deprotonation of one phenolic group and not of the enol group has been recognized as being responsible for this change.

Acknowledgment. V.G., A.M., and M.F.O. thank the Italian Ministero dell'Istruzione, dell'Università e della Ricerca. F.P. thanks the Graduate School of Engineering and the Global COE program of Tohoku University for financial support. B.K. thanks the Ministry of Science, Education and Sports of the Republic of Croatia through project 098-0982915-2945 for support of this work.

References and Notes

(1) Conney, A. H.; Lou, Y.-R.; Xie, J.-G.; Osawa, T.; Newmark, H. L.; Liu, Y.; Chang, R. L.; Huang, M.-T. *Proc. Soc. Exp. Biol. Med.* **1997**, *216*, 234.

(2) Began, G.; Sudharshan, E.; Udaya Sankar, K.; Appu Rao, A. G. *J. Agric. Food Chem.* **1999**, *47*, 4992.

(3) Leu, T.-H.; Maa, M.-C. *Curr. Med. Chem.: Anti-Cancer Agents* **2002**, *2*, 357.

(4) Moos, P. J.; Edes, K.; Mullally, J.; Fitzpatrick, J. *Carcinogenesis* **2004**, *9*, 1611.

(5) Fujisawa, F.; Atsumi, T.; Ishihara, M.; Kadoma, Y. *Anticancer Res.* **2004**, *24*, 563.

(6) Yang, F.; Lim, G. P.; Begum, A. N.; Ubeda, O. J.; Simmons, M. R.; Ambegaokar, S. S.; Chen, P.; Kayed, R.; Glabe, C. G.; Frautschy, S. A.; Cole, G. M. *J. Biol. Chem.* **2005**, *280*, 5892.

(7) Ryu, E. K.; Choe, Y. S.; Lee, K.-H.; Choi, Y.; Kim, B.-T. *J. Med. Chem.* **2006**, *49*, 6111.

(8) Jasim, F.; Talib, T. *J. Therm. Anal.* **1992**, *38*, 2549.

(9) Bors, W.; Kazazic, S. P.; Michel, C.; Kortenska, V. D.; Stettmaier, K.; Klasinc, L. *Int. J. Quantum Chem.* **2002**, *90*, 969.

(10) Wright, J. S. *J. Mol. Struct. (THEOCHEM)* **2002**, *591*, 207.

(11) Sun, Y.-M.; Zhang, H.-Y.; Chen, D.-Z.; Liu, C.-B. *Org. Lett.* **2002**, *4*, 2909.

(12) Sun, Y.-M.; Wang, R.-X.; Yuan, S.-L.; Lin, X.-J.; Liu, C.-B. *Chinese J. Chem.* **2004**, *22*, 827.

(13) Kolev, T. M.; Velcheva, E. A.; Stamboliyska, B. A.; Spiteller, M. *Int. J. Quantum Chem.* **2005**, *102*, 1069.

(14) Shen, L.; Ji, H.-F.; Zhang, H.-Y. *Chem. Phys. Lett.* **2005**, *409*, 300.

(15) Balasubramanian, K. *J. Agric. Food Chem.* **2006**, *54*, 3512.

(16) Shen, L.; Ji, H.-F. *Spectrochim. Acta* **2007**, *67A*, 619.

(17) Balasubramanian, K. *Int. J. Quantum Chem.* **1990**, *37*, 449.

(18) Balasubramanian, K. *Ind. J. Chem.* **1991**, *30A*, 61.

(19) Párkányi, C.; Stem-Beren, M. R.; Martínez, O. R.; Aaron, J.-J.; Bulaceanu-MacNair, M.; Arrieta, A. F. *Spectrochim. Acta A* **2004**, *60*, 1805.

(20) Klasinc, L.; Kovač, B.; Ruščić, B. *Kem. Ind. (Zagreb)* **1974**, *10*, 569.

(21) Sanche, L.; Schulz, G. J. *Phys. Rev. A* **1972**, *5*, 1672.

(22) Modelli, A.; Jones, D.; Distefano, G. *Chem. Phys. Lett.* **1982**, *86*, 434.

(23) Johnston, A. R.; Burrow, P. D. *J. Electron Spectrosc. Relat. Phenom.* **1982**, *25*, 119.

(24) Modelli, A.; Foffani, A.; Scagnolari, F.; Jones, D. *Chem. Phys. Lett.* **1989**, *163*, 269.

(25) Cederbaum, L. S. *J. Phys. B* **1975**, *8*, 290.

(26) Dunning, T. H., Jr. *J. Chem. Phys.* **1970**, *53*, 2823.

(27) Becke, A. D. *J. Chem. Phys.* **1993**, *98*, 5648.

(28) Stratmann, R. E.; Scuseria, G. E.; Frisch, M. J. *J. Chem. Phys.* **1998**, *109*, 8218.

(29) Kendall, R. A.; Dunning, T. H., Jr.; Harrison, R. J. *J. Chem. Phys.* **1992**, *96*, 6796.

(30) Barone, V.; Cossi, M.; Tomasi, J. *J. Chem. Phys.* **1997**, *107*, 3210.

(31) Frisch, M. J.; Trucks, G. W.; Schlegel, H. B.; Scuseria, G. E.; Robb, M. A.; Cheeseman, J. R.; Montgomery, J. A.; Vreven, T.; Kudin, K. N.; Burant, J. C.; Millam, J. M.; Iyengar, S. S.; Tomasi, J.; Barone, V.; Mennucci, B.; Cossi, M.; Scalmani, G.; Rega, N.; Petersson, G. A.; Nakatsuji, H.; Hada, M.; Ehara, M.; Toyota, K.; Fukuda, R.; Hasegawa, J.; Ishida, M.; Nakajima, T.; Honda, Y.; Kitao, O.; Nakai, H.; Klene, M.; Li, X.; Knox, J. E.; Hratchian, H. P.; Cross, J. B.; Bakken, V.; Adamo, C.; Jaramillo, J.; Gomperts, R.; Stratmann, R. E.; Yazyev, O.; Austin, A. J.; Cammi, R.; Pomelli, C.; Ochterski, J. W.; Ayala, P. Y.; Morokuma, K.; Voth, G. A.; Salvador, P.; Dannenberg, J. J.; Zakrzewski, V. G.; Dapprich, S.; Daniels, A. D.; Strain, M. C.; Farkas, O.; Malick, D. K.; Rabuck, A. D.; Raghavachari, K.; Foresman, J. B.; Ortiz, J. V.; Cui, Q.; Baboul, A. G.; Clifford, S.; Cioslowski, J.; Stefanov, B. B.; Liu, G.; Liashenko, A.; Piskorz, P.; Komaroni, I.; Martin, R. L.; Fox, D. J.; Keith, T.; Al-Laham, M. A.; Peng, C. Y.; Nanayakkara, A.; Challacombe, M.; Gill, P. M. W.; Johnson, B.; Chen, W.; Wong, M. W.; Gonzalez, C.; Pople, J. A. *Gaussian 03*, Revision D.01; Gaussian Inc.: Wallingford, CT, 2004.

(32) Tønnesen, H. H.; Karlsen, J.; Mostad, A. *Acta Chem. Scand.* **1982**, *B36*, 475.

(33) Mague, J. T.; Alworth, W. L.; Payton, F. L. *Acta Crystallogr.* **2004**, *C60*, 608.

(34) Payton, F.; Sandusky, P.; Alworth, W. L. *J. Nat. Prod.* **2007**, *70*, 143.

(35) Deleuze, M. S. *J. Chem. Phys.* **2002**, *116*, 7012.

(36) Deleuze, M. S. *J. Phys. Chem. A* **2004**, *108*, 9244.

(37) Deleuze, M. S. *Chem. Phys.* **2006**, *329*, 22.

(38) Mines, G. W.; Thompson, H. A. *Proc. R. Soc., Ser. A* **1974**, *342*, 327.

(39) Hush, N. S.; Livett, M. K.; Peel, J. B.; Willett, G. D. *Aust. J. Chem.* **1987**, *40*, 599.

(40) Maier, J. P.; Turner, D. W. *J. Chem. Soc., Faraday Trans. II* **1973**, 521.

(41) Kesper, K.; Münzel, N.; Pietzuch, W.; Specht, H.; Schweig, A. *J. Mol. Struct. (THEOCHEM)* **1989**, *59*, 375.

(42) Dunning, T. H., Jr.; Peterson, K. A.; Woon, D. E. Basis Sets: Correlation Consistent Sets. In *Encyclopedia of Computational Chemistry*; Schleyer, P. v. R., Ed.; Wiley: Chichester, U.K., 1998.

(43) Chen, D.; Gallup, G. A. *J. Chem. Phys.* **1990**, *93*, 8893.

(44) Staley, S. S.; Strnad, J. T. *J. Phys. Chem.* **1994**, *98*, 161.

(45) Chao, J. S-Y.; Falcetta, M. F.; Jordan, K. D. *J. Chem. Phys.* **1990**, *93*, 1125.

(46) Burrow, P. D.; Howard, A. E.; Johnston, A. R.; Jordan, K. D. *J. Phys. Chem.* **1992**, *96*, 7570.

(47) Venuti, M.; Modelli, A. *J. Chem. Phys.* **2000**, *113*, 2159.

(48) Modelli, A.; Hajgató, B.; Nixon, J. F.; Nyulászi, L. *J. Phys. Chem. A* **2004**, *108*, 7440.

(49) Modelli, A. *Phys. Chem. Chem. Phys.* **2003**, *5*, 2923.

(50) Modelli, A. *Trends Chem. Phys.* **1997**, *6*, 57.

(51) Modelli, A.; Distefano, G.; Jones, D. *Chem. Phys.* **1982**, *73*, 395.

(52) Modelli, A.; Burrow, P. D. *J. Electron Spectrosc. Relat. Phenom.* **1983**, *32*, 263.

(53) Zsila, F.; Bikádi, Z.; Simonyi, M. *Tetrahedron: Asymmetry* **2003**, *14*, 2433.

(54) Baumann, W.; Rodrigues, S. V.; Viana, L. M. *Braz. J. Chem. Eng.* **2000**, *17*, 323.

(55) Dyrssen, D. W.; Novikov, Y. P.; Uppström, L. R. *Anal. Chim. Acta* **1972**, *60*, 139.

(56) Borsari, M.; Ferrari, E.; Grandi, R.; Saladini, M. *Inorg. Chim. Acta* **2002**, *328*, 61.

(57) Litwinienko, G. G.; Ingold, K. U. *J. Org. Chem.* **2004**, *69*, 5888.

(58) Bernabé-Pineda, M.; Ramírez-Silva, M.; Romero-Romo, M.; González-Vergara, E.; Rojas-Hernández, A. *Spectrochim. Acta A* **2004**, *60*, 1091.

(59) Kuo, P.-C.; Damu, A. G.; Cherng, C. Y.; Jeng, J. F.; Teng, C. M.; Lee, E.-J.; Wu, T.-S. *Arch. Pharm. Res.* **2005**, *28*, 518.

(60) Kwasniewski, S. P.; Deleuze, M. S.; François, J. P. *Int. J. Quantum Chem.* **2000**, *80*, 672.

(61) Hsu, C.-P.; Hirata, S.; Head-Gordon, M. *J. Phys. Chem. A* **2001**, *105*, 451.

(62) Chignell, C. F.; Bilski, P.; Reszka, K. J.; Motten, A. G.; Sik, R. H.; Dahl, T. A. *Photochem. Photobiol.* **1994**, *55*, 295.

(63) Tønnesen, H. H.; Arrieta, A. F.; Lerner, D. *Pharmazie* **1995**, *50*, 689.

(64) Khopde, S. M.; Priyadarsini, K. I.; Palit, D. K.; Mukherjee, T. *Photochem. Photobiol.* **2000**, *72*, 625.

(65) Bong, P.-H. *Bull. Korean Chem. Soc.* **2000**, *21*, 81.

(66) Wright, J. S.; Rowley, C. N.; Chepelev, L. L. *Mol. Phys.* **2005**, *103*, 815.